LTCC-Based Sensors for Mechanical Quantities

Uwe Partsch[1], Christian Lenz[1], Steffen Ziesche[1], Carolin Lohrberg[1], Holger Neubert[2], Thomas Maeder[3]

[1] Fraunhofer IKTS, Dresden, Germany
[2] Technische Universität Dresden, Germany
[3] Laboratoire de Production Microtechnique, EPFL, Lausanne, Switzerland

Abstract: Besides their excellent dielectric and thermo-mechanical characteristics Low Temperature Cofiring Ceramics (LTCC) are also well suited for the fabrication of 3D micromechanical components such as sensors for mechanical quantities. This paper describes the development of such sensors covering some material and technological aspects. Furthermore, the design process for mechanical sensors is discussed as well as application examples of sensors for the detection of pressure, force, acceleration and flow.

Key words: LTCC, Sensors, 3D-Integration.

Senzorji mehanskih veličin na osnovi LTCC

Povzetek: Poleg odličnih dielektričnih in termo-mehanskih lastnosti so keramike z nizko temperaturo žganja (LTCC) primerne tudi za izdelavo 3D mikro mehanskih komponent, kot so senzorji mehanskih veličin. Članek opisuje razvoj teh senzorjev vključno z nekaterimi tehnološkimi in materialnimi vidiki. Dodatno je predstavljen postopek oblikovanja mehaničnih senzorjev in nekaj primerov senzorjev tlaka, sile, pospeška in pretoka.

Ključne besede: LTCC, senzorji, 3D-integracija

* Corresponding Author's e-mail: uwe.partsch@ikts.fraunhofer.de

1. Introduction

Ceramic sensors are applied when specific requirements have to be fulfilled, e.g. a high reliability at elevated and cycled temperatures, harsh environment as well as in aggressive chemicals.

The ceramic multilayer technology (e.g. LTCC) enhances these advantages because of its ability (i) for a complex 3D miniaturization with embedded deformable bodies (cantilever, diaphragms), channels and cavities as well as the ability (ii) for the direct integration of electronic components for signal conditioning and processing.

One reason for the outstanding commercialization success of LTCC-based sensors is the cost level which is mainly defined by material and process costs. In order to reduce material and process costs, miniaturization is the most important leverage.

2. Material aspects

The manufacturing of LTCC-based 3D micro-components means the co- and post-firing of glass-ceramic layers and different functional materials. During co-firing, in particular, intensive mechanical and chemical interactions can appear, strongly influencing the component performance.

The successful processing of multilayered multi-material based miniaturized LTCC components requires the proper control of different materials and technological aspects.

2.1 LTCC

One reason that ceramic materials are advantageously used for deforming bodies in sensor applications is their linear stress vs. strain behaviour. Table 1 compares different ceramic materials in terms of their mechanical properties.

Table 1: Mechanical properties of different ceramics (CTE … coefficient of thermal expansion (20... 400°C), E …Young's modulus, σ_B … bending strength).

Material	CTE	E	σ_B	σ_B/E
	ppm/ K	GPa	MPa	10^{-3}
96% Al$_2$O$_3$ [1)]	7.6	350	310	0.9
99.8% Al$_2$O$_3$ [2)]	7.5	406	630	1.6
LTCC [3)]	5.8	120	320	2.7
YSZ [4)]	11.2	210	1050	5.0
ZTA [5)]	8.1	357	1350	3.8

Datasheet values: [1)] CeramTec V38, [2)] CeramTec RK 87, [3)] Du Pont DP 951, [4)] CeramTec MZ 429, [5)] CeramTec DC 25.

The σ_B/E ratio determines the dimension of the deforming bodies in terms of sensitivity and overload stability. The larger the σ_B/E ratio the smaller the deforming bodies can be designed. It can be seen that LTCC is well suited because of a σ_B/E ratio of 2.7. However, YSZ (σ_B/E = 5) and ZTA (σ_B/E = 3.8) have a better mechanical performance, but embedding e.g. of low sintering noble metals as well as resistors can only be realized using a low temperature firing system.

Different types of LTCC show a different bending strength behavior [1]. Best values can be obtained using the Du Pont's Green Tape 951 system (Figure 1). It must however be noted that, in order to ensure long-term reliability, static [2] and cyclic fatigue [3] must also be accounted for.
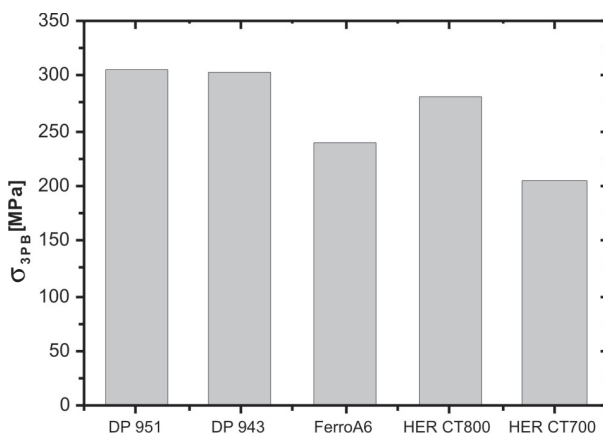

Figure 1: Comparison of different LTCC types regarding their fractural strength (re-calculated after [1]).

The 951 system offers different tape thicknesses (50 – 254 μm unfired) as well as a full system of the required pastes (inner/outer conductors, via, outer/inner resistors). This makes it particularly well suited for the fabrication of sensors.

The shrinkage control of LTCC multilayer components plays an important role regarding the final dimensional control e.g. for advanced electronic packages (chip sized packages, flip chip) but also in the case of mechanical sensors.

Shrinkage occurring during firing can be influenced by controlling the process factors (of lamination and firing). Figure 2 shows the influence of lamination temperature and pressure.
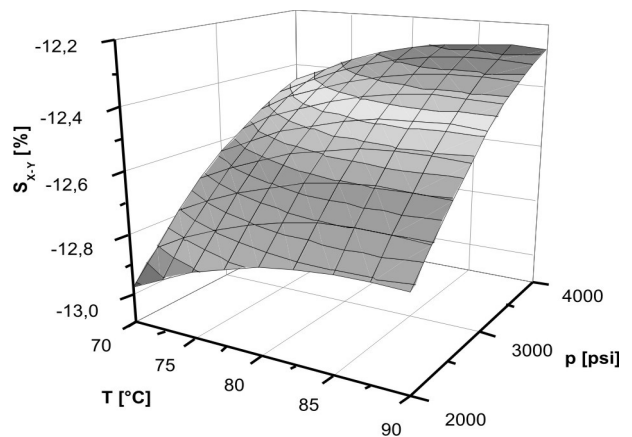

Figure 2: LTCC DP 951 X-Y shrinkage (S$_{X-Y}$) vs. lamination temperature (T) and pressure (p) [4].

2.2 Functional Thick Films

2.2.1 Metallization

In many cases, LTCC-suited inner metallization pastes are silver-based. The interaction between silver and LTCC during co-firing was described in the past by several authors e.g. [4-6], it can lead to significant warping of thin and 3D structured LTCC geometries.
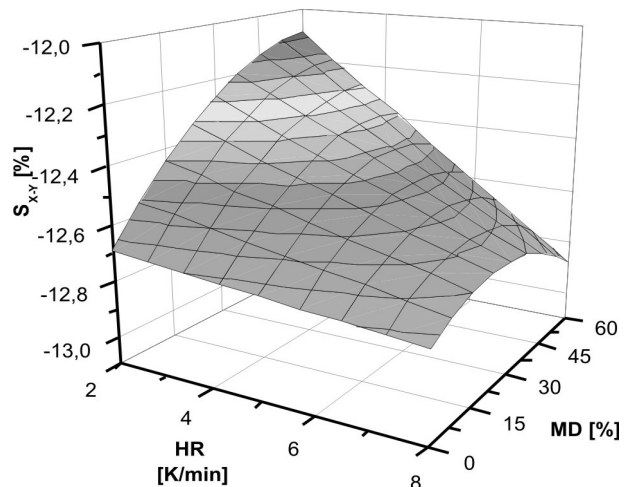

Figure 4: LTCC DP 951 X-Y shrinkage (S$_{X-Y}$) vs. heat up ramp (HR) and metallization degree (MD) [4].

Figure 4 shows that the shrinkage of a DP 951-based LTCC multilayer during firing is – in addition to the lamination parameters – also influenced by the degree of metallization and the heat up ramp. It can be seen that there is only a slight effect on the X-Y shrinkage by changing the heat up rate, when the multilayer is not metalized. In the case of an extensive metallization (60% metallization area) there is a strong dependence on the heat up ramp. The metalized multilayer shrinks in the same way as the non-metalized multilayer at higher heat up ramps (12.8% @ 8K/min). Using low heat up ramps (2 K/min), the shrinkage is reduced to 12.1%. The silver layer has a "locking" function due to the different shrinkage behavior.

Besides this pure mechanical effect there are also chemical interactions between the silver layer and the LTCC. [6] and [5] demonstrated a strong degree of silver diffusion into the LTCC, which can reach some 10 µm. [7] showed that silver influences the viscosity of the LTCC glass leading to an earlier densification and crystallization. Because silver enters the LTCC glass matrix in an oxidized status, a nitrogen sintering atmosphere can minimize the discussed effects, by shifting the chemical equilibrium between Ag^+(glass) and $Ag0$ (metal) in favour of the latter.

2.2.2 Piezo-Resistors

The transformation of a mechanical quantity into an electrical signal by piezo-resistors is one of the most common measuring principles. Using a deformable body with piezo-resistors in the areas with high mechanical strain, a mechanical input quantity (e.g. force) can be transduced into a proportional resistance/bridge voltage change (Figure 5).
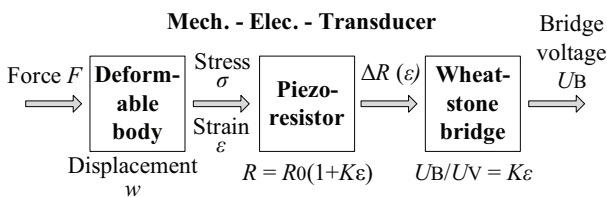

Figure 5: Sensor transmission chain [8].

Based on their microstructure and effective conducting mechanism, thick-film resistors (TFRs) always have a strain sensitive behavior.

As well as the thermal behavior, the strain sensitivity of TFRs is dominated by insulating/semi-conductive nanoscale glass layers between conducting particles, within the three-dimensional conductive chains, strain-dependent interparticle tunneling being the favoured mechanism [9, 10].

The strain sensitivity is specified using the K- or gauge factor which determines the ratio between the relative change of resistance and the applied strain.

Measured gauge factors of TFRs are between 2 and 35. They are influenced by (i) the composition of the TFR (type, grain sizes and proportion of glasses and conductive phases), (ii) the firing process (dissolution of the conductive phase into the glass), and (iii) the interactions between the TFR and the substrate as well as the terminations (diffusion of silver ions into the TFR glass matrix) [11]. The maximum signal gain of TFRs is limited by noise. Therefore, the effective signal-to-noise ratio is suitable as a normalized parameter [12]:

$$SNR_{eff}[dB] = -20 \cdot \frac{\lg U_S}{U_N} \quad . \tag{1}$$

U_s and U_N are the effective signal voltage and the peak-to-peak noise voltage. Here, US was calculated using the measured gauge factors, a supply voltage of 5 V and a relative strain of e = $2.7 \cdot 10^{-4}$ (corresponds to 50% of the maximum deflection before substrate breakage). U_N was calculated by solving the definition of the noise index (NI).
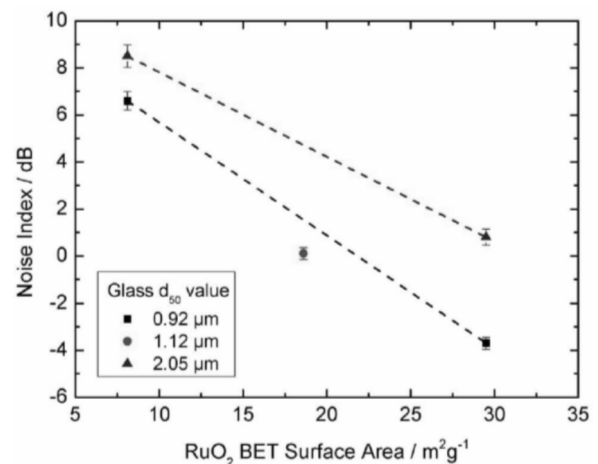

Figure 6: Strain sensor paste development [12].Noise index (NI) vs. BET surface area of RuO_2.

In order to improve the SNR_{eff} [12], compositions were developed as a mixture from RuO_2 (four different particle size distributions, one mixture) as well as two different glasses (five different particle sizes). The aim of these investigations was a TFR sheet resistance of 10 kOhm/sqr.

The results showed that the noise index (NI) and the gauge factor of TFRs are strongly influenced by the particle size distribution of the glasses as well as the conductive phase. Figures 6 and 7 illustrate that there is a

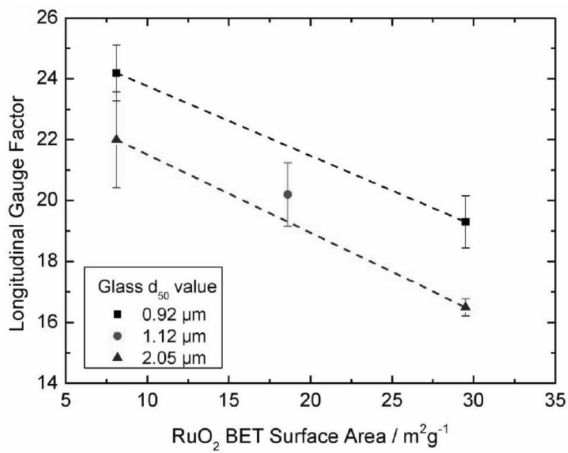compromise between gauge factor and noise behavior of TFRs.

Figure 7: Strain sensor paste development [12]. Longitudinal gauge factor vs. BET surface area of RuO_2.

However, these developments cannot improve the DP 2041 characteristics regarding the SNI_{eff}.

Further activities are planned concerning the development of new glass types, the optimization of firing and the analysis of alternative conductive phases (pyrochlores).
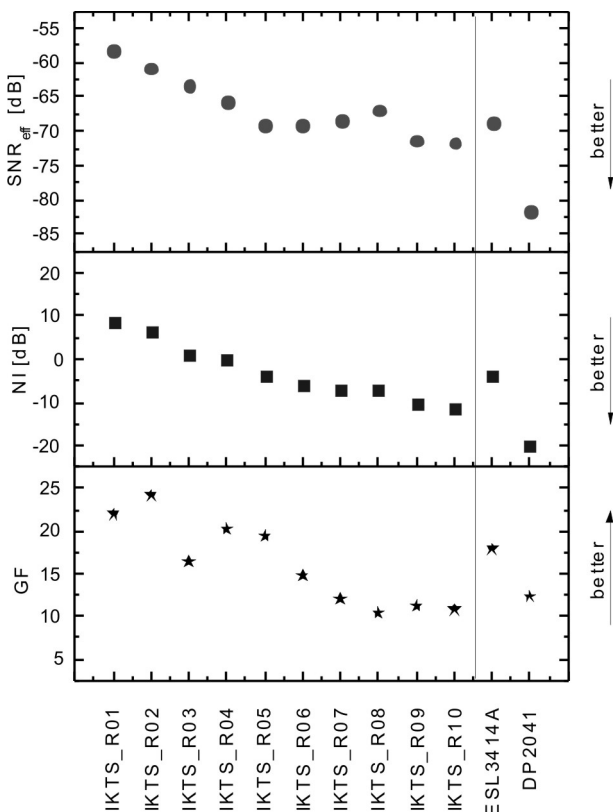

Figure 8: Effective signal-to-noise ratio (SNReff) [12]. Comparison of IKTS and commercial pastes.

2.2.3 Sacrificial Materials

Sacrificial materials temporarily stabilize functional elements during lamination and sintering. They are removed during or after sintering. Two types of sacrificial materials are differentiated:
- Mineral sacrificial paste (MSP),
- Fugitive sacrificial paste (FSP).

MSP consists of glass, an active substance and vehicle [13, 14]. The active substance is a mineral filling material. After sintering, the MSP provides a solid layer and can be removed with aqueous acetic acid. MSP suits well for cantilevers and freestanding structures with high level requirements regarding the accuracy. Closed structures are difficult to handle as MSP has to be dissolved with acid.

FSP consists of organic and graphite powder and contains no glass phases [15, 16]. The graphite is oxidized to carbon dioxide at about 700 °C. Thus, it is well suited for closed cavities, channels and diaphragms in LTCC because FSP volatilizes through the porous LTCC or open channels during sintering [15].

In order to stabilize embedded mechanical structures during sintering, FSP oxidation must be prevented using a non-oxidizing sintering atmosphere (e.g. nitrogen). In this case, a "vent" is required for out gassing the carbon dioxide from the embedded structures. The appropriate timing for the change from oxygen to nitrogen and vice versa is a critical issue. It was studied for DP 951 in [17].

The resulting profile is shown in Figure 9. The amount of FSP and the geometry of the embedded structures require an adjustment of the sintering procedure for every component to avoid warping and FSP residue effects.
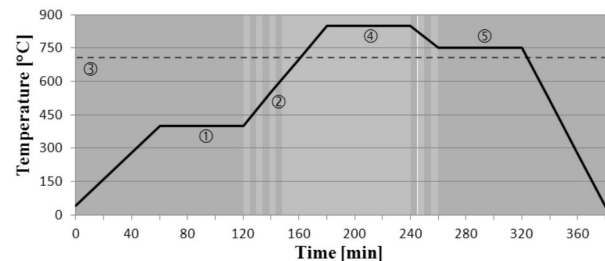
① ... Debindering: 350 °C to 550 °C
② ... Glasmelt: 650 °C to 825 °C
③ ... Carbonoxidation: 700 °C
④ ... Sintering: 850 °C
⑤ ... Burning FSP: 750 °C

Oxygen atmosphere: 10 slm
Nitrogen atmosphere: 40 slm
Transition between oxygen and nitrogen and between nitrogen and oxygen, respectively

Figure 9: Customized sintering profile for surviving FSP after sintering DP 951 [17].

However, sacrificial materials often require the application of zero-shrinkage techniques [18] because of their unadapted shrinkage behavior in comparison to standard LTCC materials.

3. Technological aspects

The higher functional integration in multilayer-based sensors and microsystems complicates their processing compared to that of multilayer substrates for electronic assemblies. Sensors for mechanical quantities, in particular, need (i) functional structures like freestanding deforming bodies, fluidic channels or heating bridges which have to be processed with no sagging or warping, (ii) deforming bodies with reinforced regions for seismic masses or force application, and (iii) low dimensional tolerances of the processed substrates to provide low variances of the performance of the fabricated sensor elements. It is a challenge to customize the standard LTCC technology for these aspects. However, the technology varies according to design, material and dimension of the sensor elements.

3.1 Sagging and warping

Sagging and warping are mainly caused by the lamination and sintering process. Below, some techniques are mentioned in order to reduce these imperfections:
- Cold lamination (uniaxial) at 30 °C reduces sagging.
- An isostatic pre-lamination of the unstructured tapes provides higher stability for the following processes like lamination. However, higher pressure ranges will then be necessary in the following lamination steps.
- A differential shrinkage of several single layers can be achieved by pre-laminating which helps to minimize sagging effects at thin deforming elements (diaphragms, cantilevers) during firing (Figure 10).
- Fixation and support of freestanding structures during sintering reduces sagging. Outer structures can be directly supported on the sintering support. Embedded structures have to be stabi-
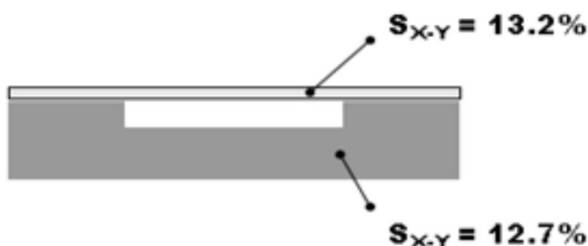
lized using additional layers like MSP or FSP. Customized sintering profiles should then be applied.
- Customized sintering profiles for integrated thick-film metallization reduce warping.

3.2 Structural elements for reinforcement

Some devices require deforming bodies with reinforced structures to supply flexural resistant properties (e.g. accelerometers or force sensors). For a precise and reproducible fabrication special techniques were established to process these bodies in multilayer technology:
- Little bars fix the reinforced regions to the outer frame during stacking and laminating (Figure 11). After laminating or sintering, these bars have to be removed by laser cutting. However, it must be considered that no other functional structures are placed under the bars which might be damaged by the laser.
- Reinforcing layers, e.g. reinforced centers of diaphragms, can also be stacked separately, as shown in Figure 11. However, this technique requires a customized stacking tool and the process gets more complex.
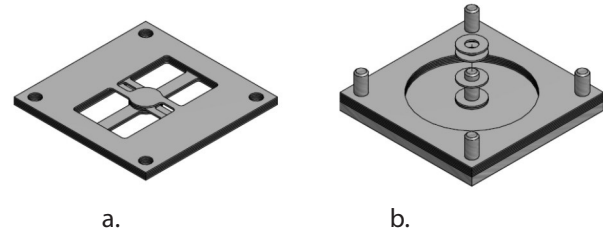

a.   b.

Figure 11: Techniques for reinforced regions: a) Fixing bars which are removed after laminating or sintering; b) separate stacking
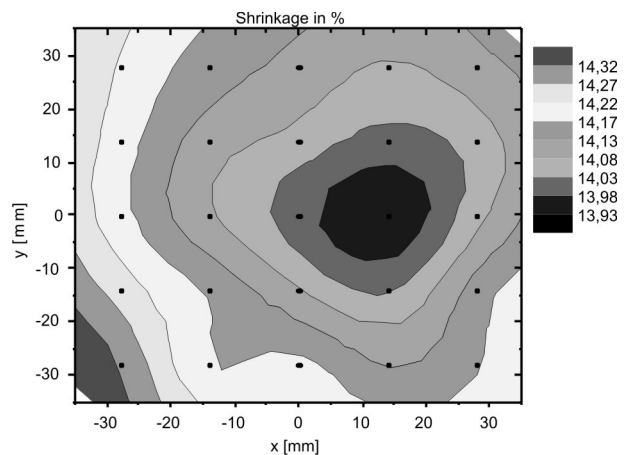
3.3 Dimensional tolerances

Figure 12: Different shrinkage of a DP 951 4-inch substrate - interpolation between 25 data points.

Figure 10: LTCC diaphragm: Different pre-lamination steps can minimize sagging effects.

Design miniaturization together with panel production of LTCC microsystems offers low-cost applications. This is one of the advantages of the LTCC technology.

However, small dimensional tolerances have to be met in order to provide reproducible properties of the sensors and to achieve an acceptable yield:

- Low tolerances have to be ensured for the structuring processes (punching, laser structuring, screen printing and stacking) over the whole working space of a multiple printed panel.
- The lamination process has to be controlled (e.g. plan parallelism at the uniaxial lamination press) to ensure homogeneous results.
- The nominal shrinkage varies over the fired substrate up to 0.5% (Figure 12). It depends on the lamination process, the structures [19] and the sintering process. For best results, the variation of the shrinkage over the working space of the panel has already to be considered in the CAD files during the design phase.

4. Sensor design

Even though the LTCC technology provides many different applications for mechanical sensors, the general design process is almost the same (Figure 13).
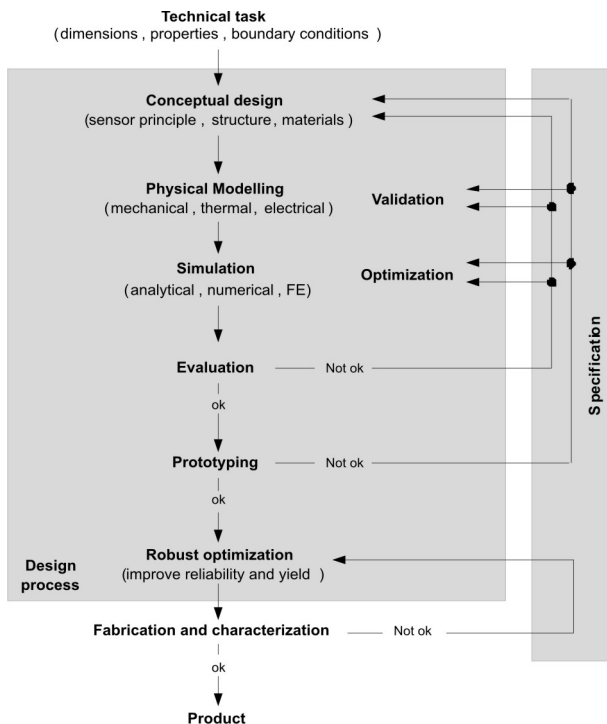

Figure 13: General design process for mechanical sensors in LTCC.

At the beginning, technical specifications have to be defined (e.g. sensor properties, dimensions and boundary conditions).

Following that, the conceptual design must be specified regarding producibility of structures and useability of materials. After evaluation and selection, the most suitable conceptual design has to be designed in detail.

Today, model-based design and design optimization is inevitable when designing integrated sensors for mechanical quantities. Therefore, physical models of adequate levels of abstraction (granularity) have to be provided for the conceptual design and the final design step as well.

Afterwards, the final design has to be checked and revised if necessary regarding the required properties. For this purpose, an evaluation step follows which includes fabrication and characterization of prototypes. In case of unsatisfying properties, one or more development loops have to be passed to adapt sensor concept and design and to validate or improve the simulation models as well.

Technology-inherent distributions of dimensions, material properties and process parameters lead to performance variations of a set of sensors even when they all are of the same design and fabrication processes. Performance distributions can be minimized by a further design step which involves the probability distributions of the design and process parameters.

The objective of a so-called robust design optimiziation is to find a design that fulfills the target requirements specified with minimized scattering of the sensor performance [20, 21]. As a result, an improved yield is to be expected.

5. Applications

5.1 Pressure Sensor

Integrated LTCC-based pressure sensors have many advantages in comparison to classic steel or ceramic-based pressure sensors [22-24] because of the technology-inherent features.

The LTCC technology enables easily variable sensor geometries e.g. different diaphragm thicknesses for different pressure ranges by using different tape thicknesses. All types of pressure sensors (relative, absolute, differential) can be built up. Furthermore, all components of the sensor system (sensor body, pressure con-

nectors/micro piping, and electronic components) can be integrated in the LTCC-based multilayer component.
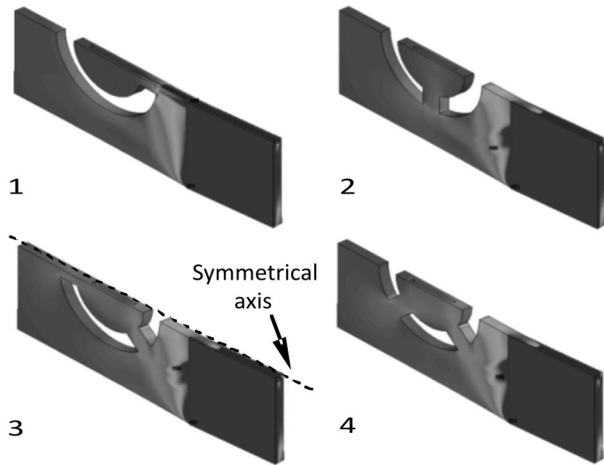

Figure 14: Finite elements analyses of different constructional designs (numbers of fixation cantilever): perfect mechanical decoupling of the sensor cell with one or two fixation cantilevers.

In [23] a new LTCC-based pressure sensor concept was presented aiming the improved mechanical decoupling of the diaphragm. The sensor cell is fixed by thin LTCC cantilevers containing micro channels for the pressure connection of the sensor cell.

Using the piezo-resistive measuring principle the strain caused by diaphragm deflection is measured by thick-film resistors, connected to a Wheatstone bridge and screen printed at the surface of the LTCC diaphragm.

FE analyses were carried out for the optimization of the design of the LTCC fixation cantilever [Figure 4].
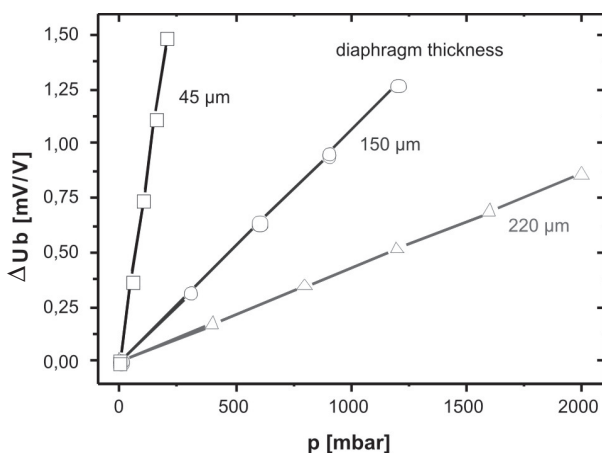

Figure 15: Characteristic curves of different sensors (pressure ranges). Shift of bridge voltage (ΔU_b) vs. applied pressure (p).

The sensor characterization showed that all sensors have a strongly linear behavior (bridge voltage vs. pressure) and are nearly free of hysteresis (Figure 15).

Table 2 shows the overall characteristics of the sensors for different pressure ranges (0.2, 1.5, 5 bar nominal pressure). The operation pressure of the different sensors was defined by additional burst tests. All sensors have a 4-times overload safety.

Table 2: Characteristics of different sensor types according to DIN/ISO 16086 (offset voltage < 25 mV/V, bridge resistance ~ 25 kOhm, T=25 °C). D – diaphragm diameter, d – diaphragm thickness, p_{op} – operation pressure, S – sensitivity, L – linearity, H – hysteresis; FS – full scale.

Diaphragm		p_{op}	S	L	H
D [mm]	d [µm]	[bar]	[mV/ V×bar]	[%FS]	[%FS]
4.5	220	5.0	0.4	0.06	0.05
4.5	150	1.5	1.1	0.04	0.01
4.5	45	0.2	4.6	0.07	0.08

Finally, sensors with integrated signal conditioning electronics (amplifier, temperature compensation) were fabricated (Figure 16).
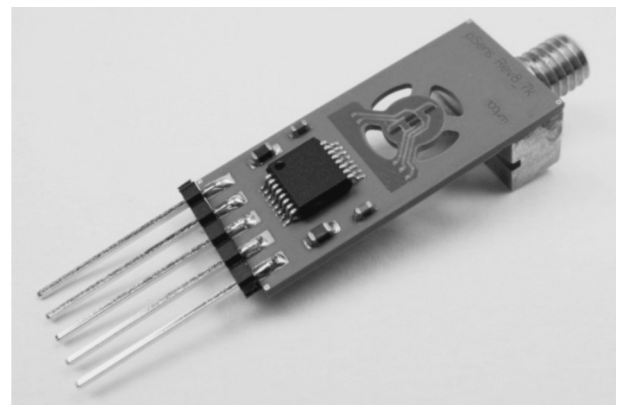

Figure 16: LTCC pressure sensor with integrated electronics for signal condition.

5.2 Force Sensor

Force sensors always detect the effect (deformation, stress, strain) of an applied force on a deformable body. The deformation is converted into an electrical signal by transducers working on the principle of e.g. capacitive, piezoelectric or piezo-resistive measurements. Though, the piezo-resistive principle is best suited because of its high accuracy, long-term stability and application range. When this transducer principle is applied, cantilevers and diaphragms obtain the best performance for small nominal loads.
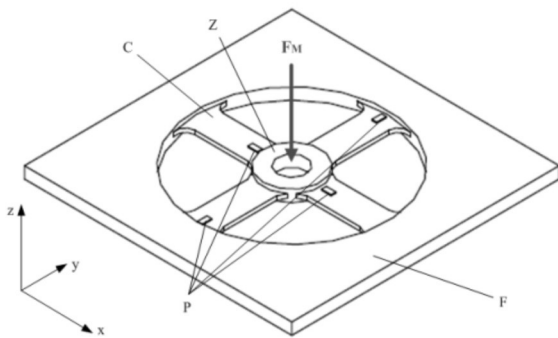
Figure 17: The cartwheel structure [8]. C - cantilever; Z - flexural resistant center; P – piezo-resistors; F - frame.

Miniaturized piezo-resistive force sensors for tensile and compressive loads (2 N, 5 N and 10 N) were developed. Compared to the pressure sensor above, the uniform application of the force to be measured in the deforming sensing body is the main challenge of this study. For this purpose, a cartwheel structure was designed (Figure 17). It consists of four identical cantilevers which are combined by a flexural resistant center. A metal pin with thread is mounted axially in the center hole. This structure obtains a uniform distribution of the applied tensile or compressive forces on the cantilevers, avoids angle errors and combines both, the high sensitivity of cantilevers and the robustness against shear forces of diaphragms.

Four piezo-resistors are placed on the cantilevers in areas of maximum strain – two under expansion and two under compression. They are connected to a Wheatstone bridge, thus the bridge voltage composes the sensing signal.
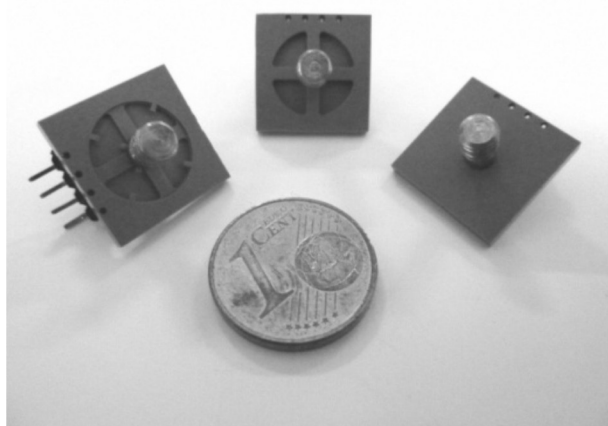

Figure 18: LTCC force sensors for three nominal loads (2 N, 5 N, 10 N). Dimensions: 14 x 14 mm^2.

An analytical model [8] was developed for the dimensioning and simulation of the sensor elements. The

most important restrictions for the design process were (i) to achieve a high grade of miniaturization, (ii) to provide robustness against overloads up to 200% of the nominal load and (iii) an equal layout for the mentioned force ranges except the top layer (Figure 18).

Table 3: Measured sensor characteristics (T = 25°C). F_B – breaking load, S – sensitivity, L – linearity, TC-S – temperature coefficient sensitivity, FS – full scale.

Nominal load F N	F_B [N]	S [mV/(V·N)]	L [%FS]	TC-S [%S/K]
2 N	4	2.6	< 0.6	0.02
5 N	> 10	0.6	< 0.4	0.03
10 N	> 20	0.1	< 1.0	0.02

The designed sensors were fabricated in multiple processing with 25 elements per 4-inch substrate. The techniques: pre-lamination of all sheets, uniaxial cold lamination at 30°C and the fixation of the deformable bodies on the sinter support were used to minimize sagging.

The measured characteristics in Table 3 show the potential of the LTCC as base material for this application. The sensors have a linear behavior and a low temperature drift of the sensitivity. Furthermore, there is a good compromise between sensitivity and breaking load.
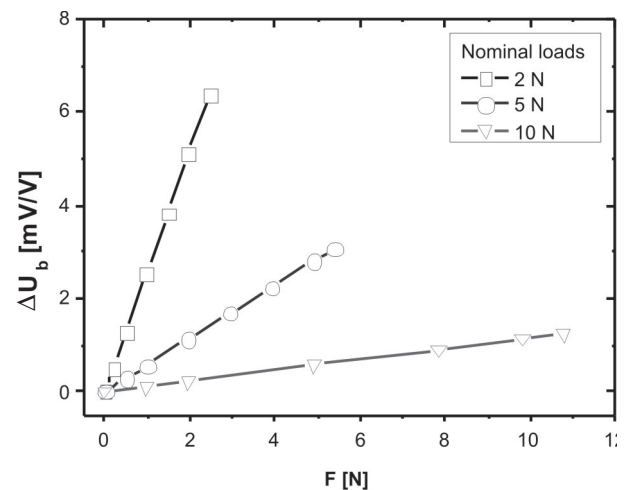

Figure 19: Characteristic curves of different sensors (load ranges). Shift of bridge voltage (ΔUb) vs. applied force (F).

5.3 Acceleration Sensor

The measurement of accelerations requires a mass element on a spring. The mass elongates and deforms the spring in response to an applied acceleration. The deformation can be measured e.g. by a piezo-resistive transducer.

Today's acceleration sensors made of silicon offer sufficient functionality in a cost-effective way. In contrast, acceleration sensors made of LTCC work under elevated temperatures, or as an additional feature integrated in LTCC substrates or electronic assemblies.

The LTCC multilayer technology suggests a sensor layout with leaf springs in a layer stressed for bending or for torsion. Thus, an acceleration perpendicular to the layer effects a deformation of the springs which can be measured by piezo-resistive thick-film resistors printed on the springs. The layout has to consider some conflicting requirements, e.g. high resonance frequency, i.e. high stiffness versus high sensitivity, i.e. lower stiffness, or uniform strain in the benders for a high reliability versus high strained areas of the springs for a high sensitivity.

Analytical and finite element models were used to optimize the sensor design. Two parallel trapezoidal benders have advantages as compared to rectangular benders or torsion springs, or the bridge and cantilever structures proposed in [25]. A FEA model of the optimized layout fabricated in LTCC is shown in Figure 20.
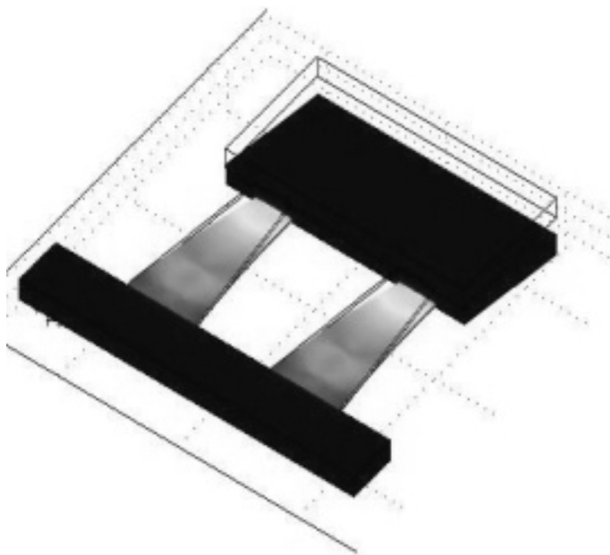
Figure 20: FEA model of an acceleration sensor with two trapezoidal benders (equivalent strain).

The first resonance frequency has a strong influence to the working range and is obtained from FEA models. A linear relation between acceleration and deformation can be expected about 50% of the resonant frequency. Resonant excitation would destroy the sensor. Four thick-film resistors, two on the benders and two on the frame are connected to a Wheatstone bridge like it has been done in case of the pressure sensors.
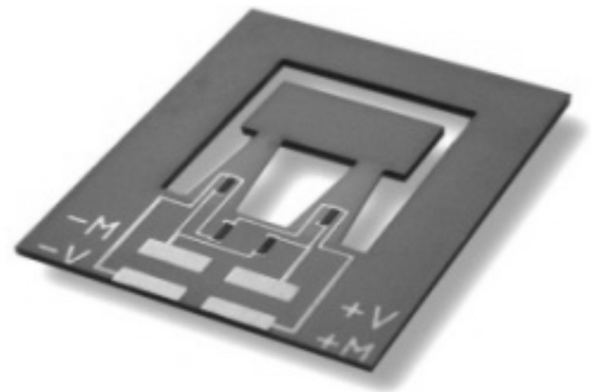
Figure 21: LTCC acceleration sensor with piezo-resistors on rectangle leaf springs.
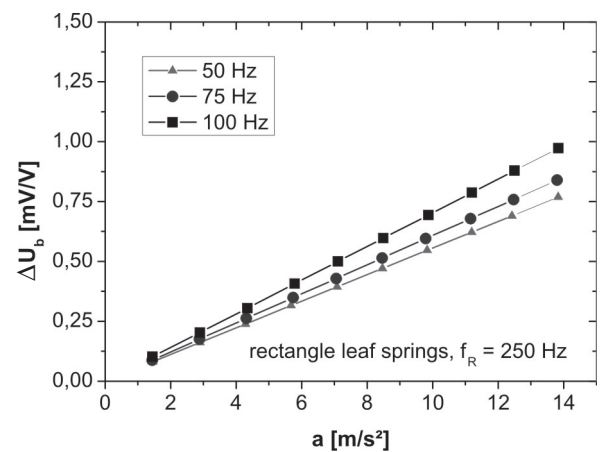
Figure 22: LTCC acceleration sensor characteristic curve, bridge voltage (U_b) vs. acceleration. Different excitation frequencies.

Figure 21 shows a LTCC acceleration sensor with a resonance frequency of 250 Hz [20]. Excited with 100 Hz the sensor gives a slightly higher signal due to the closer proximity to the resonance frequency as compared to 50 or 75 Hz (Figure 22).

However, the tested sensors are sensitive for large accelerations. Smaller effective ranges or can be designed.

5.4 Flow Sensor

Most of the commercial flow sensors work on the heating wire principle. A thin platinum wire which is heated by a current is placed in a flowing gas. It cools the platinum wire which refers to its resistance and influences the connected Wheatstone bridge. The implementation of a channel system with integrated freestanding heating wire in LTCC is only possible when using a sacrificial material. A thin heater can be realized by overprinting the FSP with a thick-film platinum paste. It enables low power loss and raises the sensitivity.

In order to reach an adjusted shrinkage between LTCC and FSP a zero-shrinkage technique is required. For this purpose, several techniques were investigated:
- The combination of DP 951 with Release-tapes (Ceramtape A, GT 951 RT) indicates delamination and residues at removal respectively.
- The self-constrained LTCC-tape HL2000 (Heraeus) is not suitable to uniaxial lamination process (voids and delamination) which is required and the FSP-paste (residues after firing).
- Best results were achieved with a combination of DP 951 and HL2000 (Figure 23). DP 951 suits to the FSP-paste and stabilizes the HL2000 during the lamination process. The zero shrinkage of the whole substrate is constrained by the HL2000.
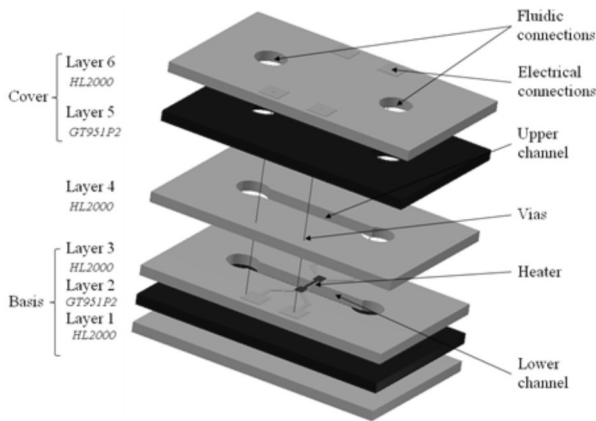

Figure 23: Explosion drawing of the LTCC flow sensor.

Figure 23 illustrates the final sensor design [Loh12]. The bottom part of the channel was filled with sacrificial material, which was overprinted by glass and platinum paste to create the heater structure.

Afterwards, the upper channel part was laminated on top of it so that the heater was centered. With this technique a lot of different heater geometries can be realized.

Table 4: Sensor characteristics. d_H – heater thickness, L_H – heater length, R_{H0} – heater resistance (T = 25 °C), R_{H100} – heater resistance (T = 100 °C).

Channel cross section A_C	d_H [μm]	L_H [mm]	R_{H0} [Ω]	R_{H100} [Ω]
0.8 mm	50	4	2.5	3.1

The prototypes show the expected relation between the current through the heating wire and the fluid flow. Figure 24 shows the characteristic curve of the sensor. In future work, a measuring circuit will be integrated in the system to complete the sensor and to linearize the current-flow correlation.
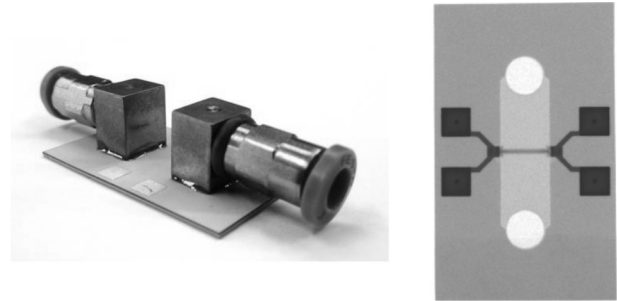
Fabricated flow sensor with assembled fluidic adapters
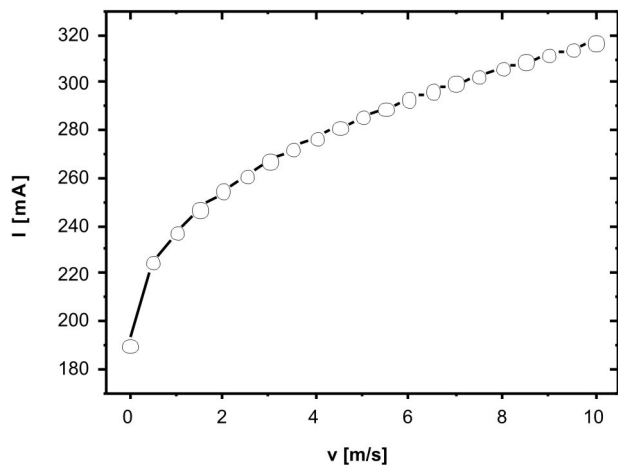
CT-scan of the fabricated flow sensor

Figure 24: LTCC flow sensor and characteristic curve, heater current (I) vs. fluid flow (v).

6. Conclusions

The selected examples show that LTCC is a well suited integration platform for mechanical sensors. Their design and fabrication requires a deep understanding and control of material issues (e.g. material interactions during co-firing, shrinkage behavior, sacrificial layer). Besides this, it is necessary to expand the LTCC process flow on the generation of the required 3D structural elements.

Pressure, force, acceleration and flow sensors were developed following a defined design and manufacturing flow.

It was shown that the sensors have an excellent and stable functionality in all cases. The main advantage of the presented sensors is the quasi-monolithic design. It prevents thermo-mechanical strain which normally occurs when parts of different materials are bonded.

Using the demonstrated material and process expansions and improvements, LTCC-based sensors for mechanical quantities are interesting and cost-effective alternatives to existing technical solutions.

References

1. Jones, W. K.; Liu, Y.; Larsen, B.; Wang, P. and Zampino, M.: "Chemical, Structural, and Mechanical Properties of the LTCC Tapes", The International Journal of Microcircuits and Electronic Packaging, Volume 23, Number 4, Fourth Quarter, 2000, S. 469.

2. Maeder, T.; Jacq, C. and Ryser, P.: "Long-term mechanical reliability of ceramic thick-film circuits and mechanical sensors under static load", Sensors and Actuators A, in press, (2012).

3. Duan, K.; Mai, Y.W. and Cotterell, B.: "Cyclic fatigue of a sintered Al_2O_3 / ZrO_2 ceramic", J. Mater. Sci., 30 [20] 5192-5198 (1995).

4. Partsch, U.: "Untersuchungen zum Schwindungsverhalten von LTCC-Multilayern" Diploma Thesis 1996, Friedrich-Schiller-Universität Jena.

5. Eberstein, M.; Rabe, T. and Schiller, W. A.: „Influences of the Glass Phase on Densification, Microstructure, and Properties of Low-Temperature Co-Fired Ceramics, Int. J. Appl. Ceram. Technol., 3 [6] 428–436 (2006).

6. Jau-Ho, J. and Chia-Ruey, C.: "Interfacial Reaction Kinetics between Silver and Ceramic-Filled Glass Substrate", J. Am. Ceram. Soc., 87 [7] 1287–1293 (2004).

7. Rabe, T.; Glitzky, C.; Naghib-Zadeh, H.; Oder, G.; Eberstein, M. and Töpfer, J.: "Silver in LTCC – Interfacial Reactions, Transport Processes and Influence on Properties of Ceramics, CICMT – Ceramic Interconnect and Ceramic Microsystems Technology, Denver 2009, Proceedings.

8. Lenz, C.; Ziesche, S.; Partsch, U.; Neubert, H.: "Low Temperature Cofired Ceramics (LTCC)-Based Miniaturized Load Cells", Proc. 35th International Spring Seminar on Electronics Technology, ISSE, Bad Aussee (2012).

9. Pike, G. E. and Seager, C. H.; Electrical Properties and Conduction Mechanisms of Ru-Based Thick Film (Cermet) Resistors, Journal of Applied Physics, 12/77, S. 5152.

10. Vionnet-Menot, S.; Grimaldi, C.; Maeder, T.; Ryser, P. and Strässler, S.: „Tunneling-percolation origin of nonuniversality: Theory and experiments", Phys. Rev.B 71 [6] 064201 (2005).

11. Prudenziati, M. (Ed.): "Handbook of Sensors and Actuators 1: Thick Film Sensors", Elsevier Science B.V., 1994.

12. Dietrich, S.; Kretzschmar, C.; Partsch, C.; Rebenklau, L.: „Reliability and Effective Signal-to-Noise Ratio of $Ru0_2$-based Thick Film Strain Gauges: The Effect of Conductive and Glass Particle Size", Electronics Technology, 2009. ISSE2009. 32nd International Spring Seminar.

13. Maeder, T.; Jacq, C.; Fournier, Y.; Ryser, P.: "Formulation and processing of screen-printing vehicles for sacrificial layers on thick-film and LTCC substrates", 32nd IMAPS – International Microelectronics and Packaging, Pultusk (2008), Proceedings.

14. Maeder, T.; Jacq, C.; Fournier, Y.; Hraiz, W.; Ryser, P.: „Structuration of zero-shrinkage LTCC using mineral sacrificial materials", 17th EMPC – European Microelectronics and Packaging Conference & Exhibition, Rimini (2009), Proceedings.

15. Birol, H.; Maeder, T.; Ryser, P.: "Application of graphite-based sacrificial layers for fabrication of LTCC (low temperature co-fired ceramic) membranes and micro-channels", J. Micromech. Microeng., 17 p. 50-60, (2007).

16. Malecha, K.; Maeder, T.; Jacq C.: "Fabrication of membranes and microchannels in low-temperature co-fired ceramic (LTCC) substrate using novel water-based sacrificial carbon pastes", Journal of the European Ceramic Society 32 (12), 3277-3286, 2012.

17. Lohrberg, C.: "Entwicklung LTCC-basierter hochempfindlicher Strömungssensoren", Diploma thesis 2012, Dresden University of Technology.

18. Rabe, T.; Schiller, W. A.: „Zero Shrinkage of LTCC by Self-Constrained Sintering", Int. J. Appl. Ceram. Technol., 2 [5] p. 374-382, (2005).

19. Wagner, M.: „Prozessparameter und ihr Einfluss auf die Schwindungsgenauigkeit von hochintegrierten keramischen Mehrlagenschaltungen", Diss. Thesis of University Erlangen-Nuremberg.

20. Neubert, H.; Partsch, U.; Fleischer, D.; Gruchow, M.; Kamusella, A.; Pham, T.: "Thick Film Accelerometers in LTCC-Technology – Design Optimization, Fabrication, and Characterization", IMAPS Journal of Microelectronics and Electronic Packaging 5 (2008) 4, 150-155.

21. Neubert, H.: Uncertainty-Based Design Optimization of MEMS/NEMS. In Gerald Gerlach, Klaus Wolter (Eds.): Bio and Nano Packaging Techniques for Electron Devices - Advances in Electronic Device Packaging 123. Springer 2012. pp. 119-140

22. Slosarcik, S; Bansky, J.; Dovica, M.; Tkac, M.: Unconventional Application of Low Temperature Cofired Ceramics for (Under-) Pressure Sensors, J. Electrical Engineering, (48) 1997, Nr. 9-10

23. Partsch, U.; Gebhardt, S.; Arndt, D.; Georgi, H.; Neubert, H.; Fleischer, D. and Gruchow, M.: „LTCC-

Based Sensors for Mechanical Quantities", CICMT – Ceramic Interconnect and Ceramic Microsystems Technology, Denver 2009, Proceedings.

24. Fournier, Y.; Maeder, Th.; Boutinard-Rouelle, G.; Barras, A.; Craquelin, N. and Ryser, P.: "Integrated LTCC Pressure/ Flow/ Temperature Multisensor for Compressed Air Diagnostics", *Sensors* 2010, *10*(12), 11156-11173.

25. Thelemann, T.: Die LTCC-Technologie als Basis von sensorischen, aktorischen und fluidischen Komponenten für Mikrosysteme, Diss. thesis of Ilmenau University of Technology 2005